Numerical stress analysis of tubular joints

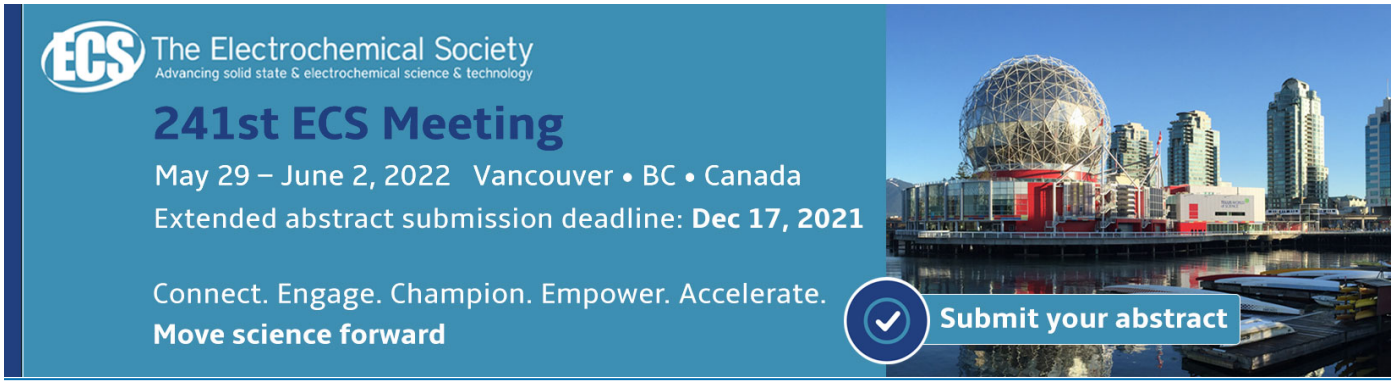

Numerical stress analysis of tubular joints

A Santacruz* and O Mikkelsen

Department of Mechanical and Structural Engineering and Material Science, Faculty of Science and Technology, University of Stavanger, Stavanger, Norway

* Contact Author: a.santacruz@stud.uis.no

Abstract. The finite element analysis (FEA) presented in this paper pertains to the stress analysis of both the welded tubular T and X joints and is aimed to assess both the importance of the presence of the weld geometry and the suitability of shell and solid elements with regards to the FEA of welded tubular joints and, additionally, to confirm or dispute a correlation between the standards AWS D1.1 and DNVGL-RP-C203 with regards to the minimum size of the weld geometry. Using symmetry, three unit-load cases are investigated: axial loading, in-plane and out-of-plane bending. The results indicate that the FE models acknowledging the presence of the weld geometry and using solid elements are more suitable for the FEA of welded tubular joints and, moreover, the stress concentration factor (SCF) obtained at the chord "crown" location from the FE models subjected to the axial load case either approach, as in the case of the welded tubular T joint, or surpass, as in the case of the welded tubular X joint, the value estimated from the parametric equations as given in DNVGL-RP-C203.

1. Introduction

Welded tubular joints of varying scale, shape, and load carrying capacity are used to build offshore structures. These joints can be loaded in any combination of three modes. These include axial loading, in-plane and out-of-plane bending. Local stresses are non-uniformly distributed due to the complexities of joint geometry and shell behaviour of welded tubular joints that control load response. Stress gradients and sites of stress concentration, especially along the brace and the chord weld toes, arise from non-uniform stress distribution. These stress concentration sites are locations where fatigue cracks can form and spread, eventually resulting in structural failure [1].

There are three basic planar joint types as shown in Figure 1 and as described below [2]:

- A Y joint consists of a chord and one brace. Axial force in the brace is reacted by an axial force and beam shear in the chord.
- A K joint consists of a chord and two braces on the same side of the chord. The components of the axial brace forces normal to the chord balance each other, while the components parallel to the chord add and are reacted by an axial force in the chord.
- An X joint consists of a chord and two braces, one on each side of the chord, where the second brace is a continuation of the first brace. Axial force in one brace is transferred through the chord to the other brace without an overall reaction in the chord.

Many joints are combinations of the aforementioned joint types, containing a variety of behaviour in one or more planes. A T joint is a Y joint in which the angle between the brace and chord is 90º. A double T joint looks like an X joint with angles of 90º but behaves as two T joints, in that the axial brace forces are transferred to the chord rather than crossing the chord to the other brace [2].

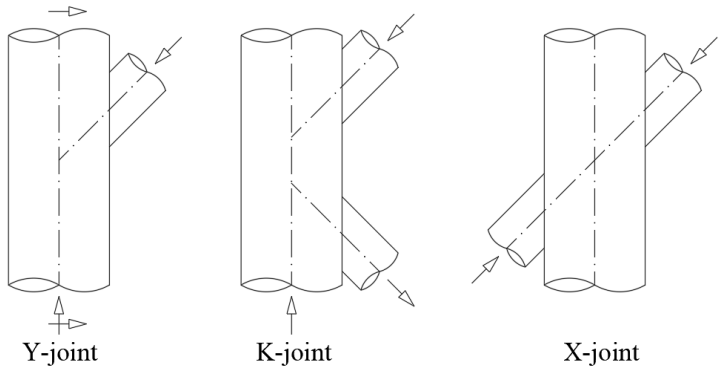

Figure 1. Basic planar joint types.

Three main sources of stress have been identified in welded tubular joints [1]:

- Nominal stresses: can be calculated using frame analysis and beam bending theory. The nature of such stresses will be determined by the joint's dimensions and the mode of loading.
- Geometric stresses: arise as a result of differences in the load response of braces and chords under the loading configuration. Geometric stresses may cause the tube wall to bend in order to ensure compatibility in the deformation of the brace and chord around the intersection.
- Notch stresses: arise from the geometric discontinuity of the tube walls introduced by an abrupt change in section at the weld toe. The greater the radius of the weld toe and the overall angle of the weld toe, the more localized deformation is limited, and the magnitude of the stresses increases. The weld toe geometry cannot be made identical for each joint configuration due to the complexity and variety of joint geometries and this creates variations in the distribution of notch stress concentrations. Consequently, it is difficult to quantify these stresses in a reliable fashion. The implementation of the hot spot stress spectrum has been adopted as a result of this.

The hot spot stress is the stress at the weld toe calculated by linear extrapolation to the weld toe of the geometric stress as shown on Figure 2. The hot spot stress excludes the contribution to the stress concentration caused by the notch effect of the weld geometry [1].

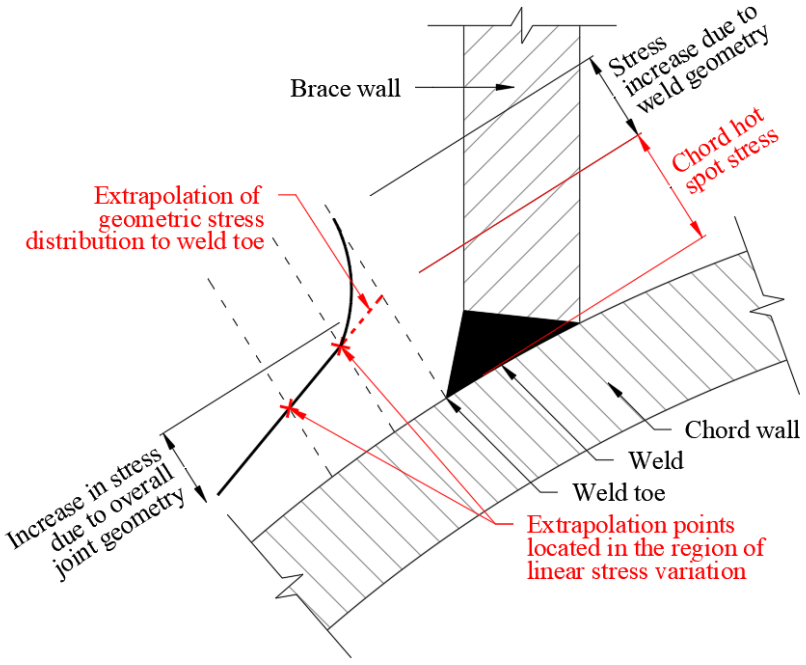

Figure 2. Schematic definition of hot spot stress in welded tubular joints.

During the design stage and during structural integrity assessment projects, assessing and measuring the hot spot stress at the intersection of welded tubular joints is an important and significant first step. There are strict guidelines regarding the location of the extrapolation points for this purpose and Figure 3 is a representation of the description as given in DNVGL-RP-C203 [3].

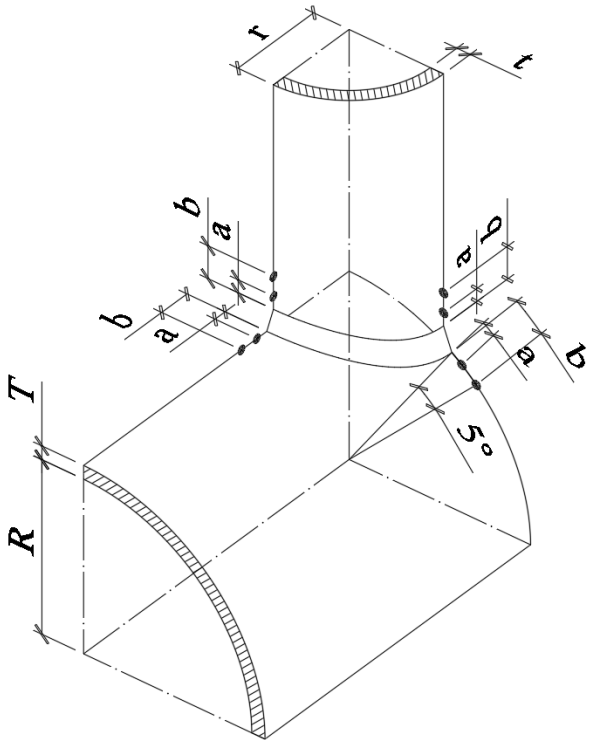

Extrapolation of stress along the brace:

$a = 0.2\ (r.t)^{1/2}$
$b = 0.65\ (r.t)^{1/2}$

Extrapolation of stress along the chord, "crown" position:

$a = 0.2\ (r.t)^{1/2}$
$b = 0.4\ (r.t.R.T)^{1/4}$

Extrapolation of stress along the chord, "saddle" position:

$a = 0.2\ (r.t)^{1/2}$
$b = 2\ \pi.R\ \frac{5}{360} = \frac{\pi.R}{36}$

Figure 3. Points for readout of stresses for extrapolation of hot spot stresses.

For the purposes of this paper, the stress distribution in the vicinity of the weld fillets on both the welded tubular T and X joints will be analysed with FE models using the general-purpose FE software "Ansys Mechanical APDL". The FEA will be performed firstly on FE models ignoring the presence of the weld geometry and, subsequently, on FE models acknowledging the presence of the weld geometry. Furthermore, the FEA will be performed using first quadrilateral isoparametric elements (shells) and, thereafter, using hexahedral isoparametric elements (solids). The weld geometry will be modelled according to the minimum requirements as recommended in AWS D1.1 [4] and, using symmetry, the FE models will be submitted to three unit-load cases: axial loading, in-plane and out-of-plane bending.

The objectives for this paper are as follows:

- To assess the importance of the presence of the weld geometry with regards to the FEA of tubular joints by comparing the results obtained from the FE models ignoring the presence of the weld geometry with those attained from the FE models acknowledging the presence of weld geometry.
- To assess the suitability of quadrilateral isoparametric elements (shells) and hexahedral isoparametric elements (solids) with regards to the FEA of welded tubular joints.
- To confirm or dispute a correlation between the standards AWS D1.1 [4] and DNVGL-RP-C203 [3] with regards to the minimum size of the weld geometry by comparing the SCFs obtained from the FEA against those estimated from the parametric equations as given in DNVGL-RP-C203 [3].

To achieve the described objectives, the results obtained from the FEA will be categorised according to the three unit-load cases implemented and analysed at the four locations of interest: the chord "crown" (CC), chord "saddle" (CS), brace "crown" (BC) and brace "saddle" (BS). In addition, it is of relevance to evaluate the FEA results against the findings reported by K. Hectors and W. De Waele [5] with regards to the importance of the presence of the weld geometry and the suitability of shell and solid elements.

2. Finite element analysis of welded tubular T and X joints

The FEA of the welded tubular T and X joints was performed using the general-purpose FE software "Ansys Mechanical APDL". The dimensions of both joint types are shown in Figure 4 and Figure 5.

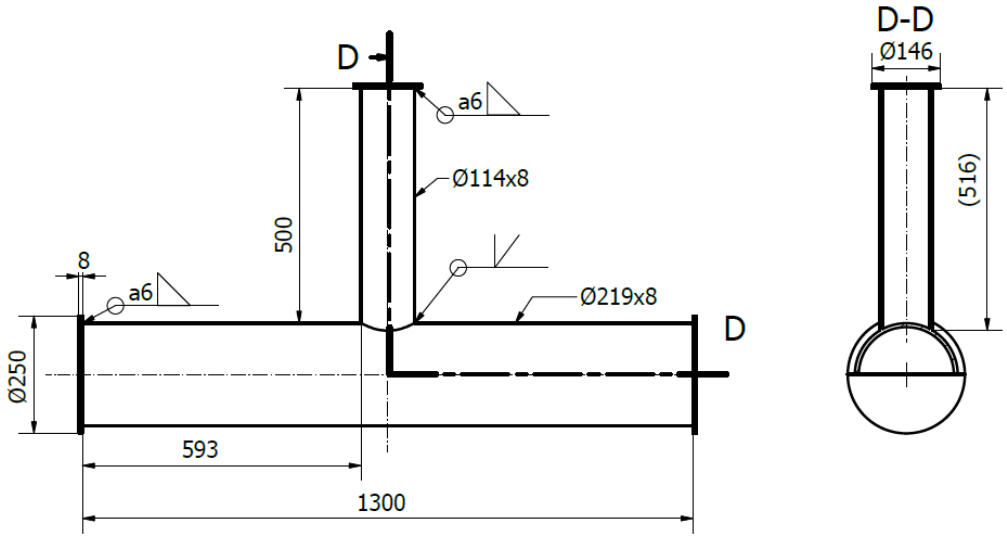

Figure 4. Dimensions of welded tubular T joint.

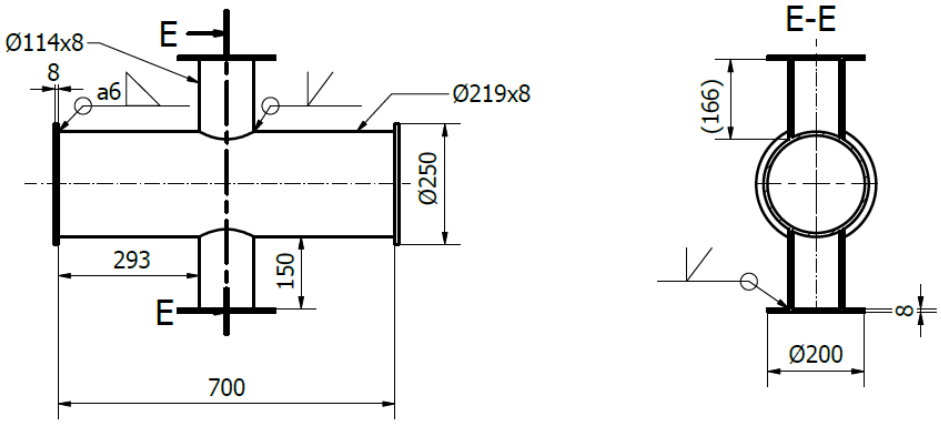

Figure 5. Dimensions of welded tubular X joint.

The material properties, as implemented in the FEA, are as follows:

- Steel designation: S355
- Modulus of elasticity: 210 GPa
- Poisson's ratio: 0.3

The weld geometry, pertaining to the FE models acknowledging the presence of the weld geometry, was modelled according to the minimum requirements as recommended in AWS D1.1-Figure 10.9 [4] and AWS D1.1-Table 10.7 [4]. For the purposes of this paper, the prequalified joint details for a complete joint penetration for groove welds in tubular T-, Y- and K-joints, as shown in AWS D1.1-Figure 10.9- "Detail B" [4], were employed to generate the weld geometry where the dihedral angle varies from 150º to 90º. The weld geometry was simplified to exclude the modelling of the weld root and include only the modelling of the weld toe. The measurements found for the weld toe locations are shown on Table 1, where the first column of the table represents the locations along the welded tubular joint intersection, 0º at the "crown" position and 90º at the "saddle" position, and the following columns show the corresponding weld toe locations for the brace and chord members.

Table 1. Weld toe locations as implemented in the FE models.

	Chord weld toe location (mm)	Brace weld toe location (mm)
0º	4.00	6.14
10º	3.92	6.06
20º	3.69	5.85
30º	3.35	5.58
40º	2.93	5.35
50º	2.50	5.21
60º	2.08	5.18
70º	1.74	5.21
80º	1.51	5.26
90º	1.42	5.29

The FE models using shell elements were specified with the first order element "SHELL181" [6] which is a four-node element with six degrees of freedom per node: x, y, and z translations, and rotations about the x, y, and z-axes. The FE models using solid elements were defined with the second order element "SOLID186" [6] which is a twenty-node element with three degrees of freedom per node: x, y and z translations. Both elements were implemented with a full numerical integration method.

Small overlaps and voids in the element model may occur when modelling with shell elements, resulting in an incorrect representation of the volume [7]. To minimize the voids and overlaps along the welded tubular joint intersections of the FE models using shell elements, a midplane section offset for both the brace member and the weld geometry and a top plane section offset for the chord member were defined as shown in Figure 6. The shell sections were applied in accordance with *Ansys Mechanical APDL Documentation, Structural Analysis Guide,* 2020 [8], "13. Shell Analysis and Cross Sections".

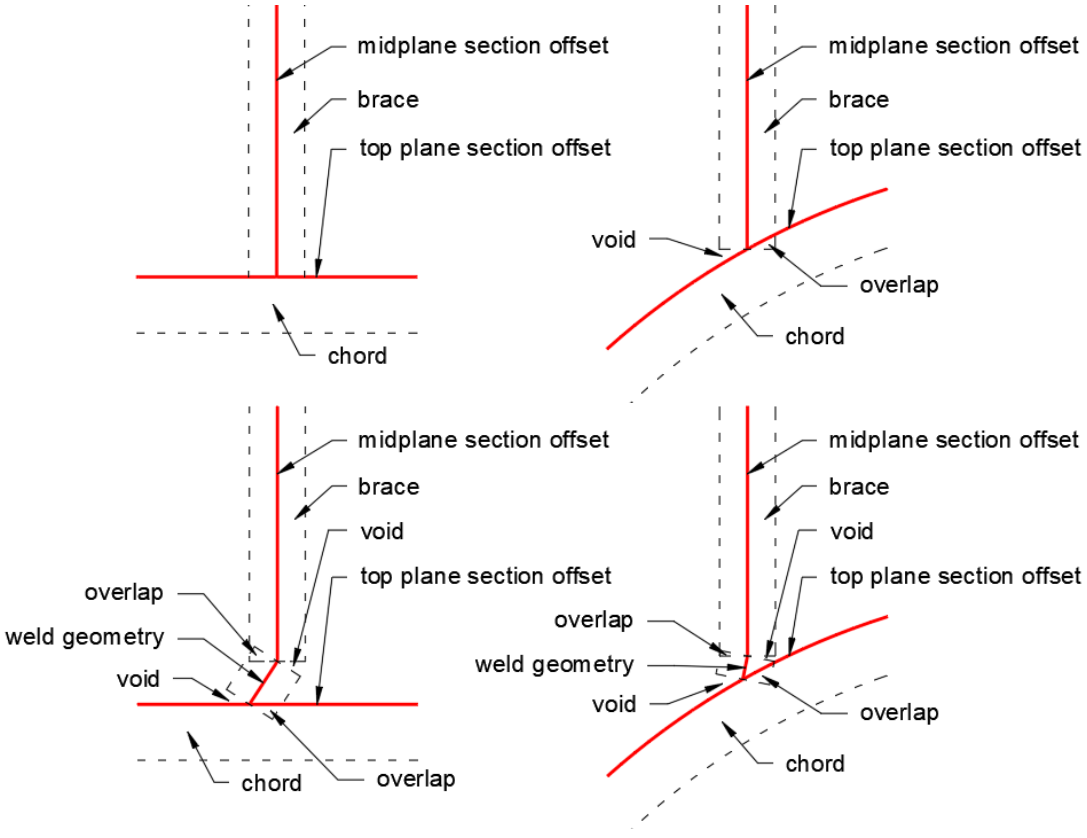

Figure 6. Overlaps and voids using shell elements.

Because of the presence of high stress gradients at the weld toe locations around the intersection of the brace and chord members, the numerical results for all three load cases are strongly mesh dependent. The approximation is easily improved by grading the mesh so that more elements appear where field gradients are high [9]. Consequently, the geometry of the FE models was sectioned to ensure a gradual mesh refinement considering the need for a denser mesh near the intersection of the brace and chord members and the need for the extrapolation points required to calculate the hot spot stresses. The FE models using shell elements were meshed with quadrilateral elements while the FE models using solid elements were meshed with hexahedral elements. Figure 7 shows a detail of the mesh at the "saddle" position as implemented in the FE models of the welded tubular T joint using solid elements and acknowledging the weld geometry where five elements were implemented through the thickness of both the brace and chord members in order to ensure mesh convergence. Mesh convergence was evaluated by comparing the "Nodal solution 1st principal stress" with the "Element solution 1st principal stress".

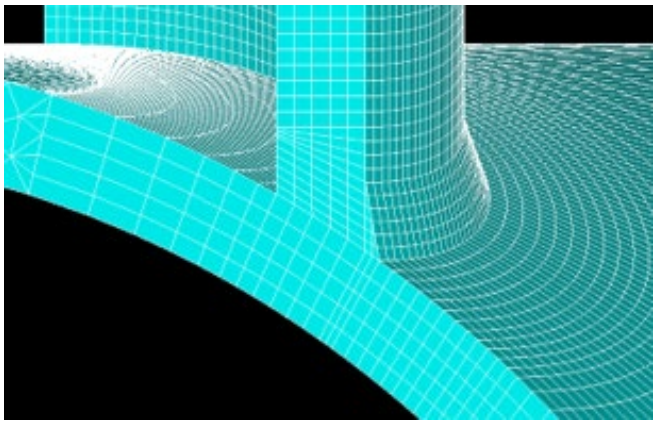

Figure 7. Detail of the mesh at the "saddle" position.

The extrapolation points were located as specified in DNVGL-RP-C203 [3]. The resulting locations "a" and "b" along the brace and chord members are shown on the second to fifth columns of Table 2. The locations "b" along the chord member are obtained by linear interpolation of the values for the "crown" and "saddle" positions. The specific locations along the welded tubular joint intersection are as shown on the first column, where 0º represents the "crown" position and 90º the "saddle" position.

Table 2. DNVGL-RP-C203, locations for extrapolation points "a" and "b".

	Chord member (mm)		Brace member (mm)	
	"a"	"b"	"a"	"b"
0º	4.27	10.06	4.27	13.88
10º	4.27	10.00	4.27	13.88
20º	4.27	9.94	4.27	13.88
30º	4.27	9.89	4.27	13.88
40º	4.27	9.83	4.27	13.88
50º	4.27	9.78	4.27	13.88
60º	4.27	9.72	4.27	13.88
70º	4.27	9.67	4.27	13.88
80º	4.27	9.61	4.27	13.88
90º	4.27	9.56	4.27	13.88

The FE models were subjected to a fixed support boundary condition placed at both ends of the chord member. The fixed support boundary conditions were applied in accordance with *Ansys Mechanical APDL Documentation, Contact Technology Guide,* 2020 [10], "10.3. Surface-Based Constraints".

The FE models were subjected to the three unit-load cases applied at the upper end of the brace member in the case of the welded tubular T joint and at the ends of both brace members in the case of the welded tubular X joint. In the case of the welded tubular X joint the load application produces a self-balancing effect. The three unit-load cases were applied in accordance with *Ansys Mechanical APDL Documentation, Contact Technology Guide,* 2020 [10], "10.3. Surface-Based Constraints".

The nominal stresses were calculated using the Euler-Bernoulli beam theory as shown on Table 3.

Table 3. Euler-Bernoulli beam theory, nominal stresses.

Normal stress due to axial load:	$\sigma_N = 3.75\ (10^{-4})\ MPa$
Bending stress due to in-plane and out-of-plane bending:	$\sigma_B = 1.52\ (10^{-5})\ MPa$

The nominal stresses were evaluated by plotting the nodal "Y-Component of stress" on a horizontal plane located 200 mm below the top of the brace member. Consequently, the results from the FEA were validated by comparing the nominal stresses obtained from the FE models with those estimated from the Euler-Bernoulli beam theory.

For the purposes of this paper, the parametric equations from Efthymiou, *Development of SCF Formulae and Generalised Influence Functions for use in Fatigue Analysis*, published in 1988, have been adopted as given in DNVGL-RP-C203 [3] and the results for both the welded tubular T and X joints are given in Table 4 and Table 5.

Table 4. DNVGL-RP-C203, SCFs for welded tubular T joint.

	CC	CS	BC	BS
Axial load:	4.68	15.52	2.38	9.47
In-plane bending:	4.14	------	3.09	------
Out-of-plane bending:	------	10.98	------	7.31

Table 5. DNVGL-RP-C203, SCFs for welded tubular X joint.

	CC	CS	BC	BS
Axial load:	3.18	22.02	2.38	12.15
In-plane bending:	4.14	------	3.09	------
Out-of-plane bending:	------	10.33	------	6.88

The geometrical parameters: $\beta = \frac{d}{D} = 0.5$, $\alpha = \frac{2L}{D} = 12$, $\gamma = \frac{D}{2T} = 14$, $\tau = \frac{t}{T} = 1$ and $\theta = 90°$ as described in DNVGL-RP-C203 [3], which are derived from the dimensions of both the welded tubular T and X joint types presented in Figure 4 and Figure 5, complied with the validity range required for the viability of the parametric equations as specified in DNVGL-RP-C203 [3].

The 1st principal stresses, extracted from the nodes for the extrapolation points "a" and "b" on both the brace and chord members, were employed to calculate the SCFs obtained from the FEA.

3. Comparison of results

The results showed that the FE models using the first order shell elements achieved an acceptable mesh convergence between the nodal and the element solution with an average of 2.7%, while the FE models using the second order solid elements achieved a higher mesh convergence between the nodal and the element solution with an average of 0.1%. Additionally, all the FE models analysed in this paper agreed with the nominal stresses calculated with the Euler-Bernoulli beam theory.

The FEA of both the welded tubular T and X joints showed that the results obtained from the FE models subjected to the in-plane bending load case displayed a maximum hot spot stress value whose location is shifted to intermediate positions between the "crown" and "saddle" locations on both the brace and chord members. The actual positions vary in relation to the type of tubular joint and the choice of element used in the analysis and to whether the presence of the weld geometry was implemented.

3.1. Comparison of results from FE models ignoring and acknowledging weld geometry

The results shown on Table 6 demonstrate that, for all the three load cases and at all the locations of interest, the FE models acknowledging the presence of weld geometry displayed higher SCFs than those obtained from the FE models ignoring the presence of weld geometry. Furthermore, the variation in the values as percentage change is higher at the brace and chord "crown" locations where the SCFs achieved their lowest values. See Appendix *"A.1. Plots-results from FE models ignoring and acknowledging weld geometry"* for a graphical illustration of the extrapolated hot spot stresses for this set of FE models.

Table 6. Results-T joint-FE models ignoring and acknowledging weld geometry, SCFs.

	CC	CS	BC	BS
DNVGL-RP-C203:	4.68	15.52	2.38	9.47
T-shell-axial:	4.49	14.47	1.19	7.13
T-shell-axial-weld:	4.76	14.80	1.20	7.40
T-solid-axial:	4.27	14.08	1.03	7.98
T-solid-axial-weld:	4.64	14.29	1.18	8.34
DNVGL-RP-C203:	4.14	------	3.09	------
T-shell-in plane bending:	2.96	------	1.40	------
T-shell-in plane bending-weld:	3.33	------	1.79	------
T-solid-in plane bending:	2.96	------	1.22	------
T-solid-in plane bending-weld:	3.32	------	1.70	------
DNVGL-RP-C203:	------	10.98	------	7.31
T-shell-out of plane bending:	------	10.19	------	5.00
T-shell-out of plane bending-weld:	------	10.27	------	5.09
T-solid-out of plane bending:	------	9.88	------	5.36
T-solid-out of plane bending-weld:	------	9.91	------	5.49

3.2. Comparison of results from FE models using shell and solid elements

The results shown on Table 7 and Table 8 demonstrate that, for all the three load cases, the SCFs obtained from the FE models using the second order solid elements are lower than those obtained from the FE models using the first order shell elements at the chord "crown", chord "saddle" and brace "crown" locations, as opposed to the SCFs obtained at the brace "saddle" location where the opposite occurs. See Appendix *"A.2. Plots-results from FE models using shell and solid elements"* for a graphical illustration of the extrapolated hot spot stresses for this set of FE models.

Table 7. Results-T joint-FE models using shell and solid elements, SCFs.

	CC	CS	BC	BS
DNVGL-RP-C203:	4.68	15.52	2.38	9.47
T-shell-axial-weld:	4.76	14.80	1.20	7.40
T-solid-axial-weld:	4.64	14.29	1.18	8.34
DNVGL-RP-C203:	4.14	------	3.09	------
T-shell-in plane bending-weld:	3.33	------	1.79	------
T-solid-in plane bending-weld:	3.32	------	1.70	------
DNVGL-RP-C203:	------	10.98	------	7.31
T-shell-out of plane bending-weld:	------	10.27	------	5.09
T-solid-out of plane bending-weld:	------	9.91	------	5.49

Table 8. Results-X joint-FE models using shell and solid elements, SCFs.

	CC	CS	BC	BS
DNVGL-RP-C203:	3.18	22.02	2.38	12.15
X-shell-axial-weld:	4.81	15.04	1.40	7.57
X-solid-axial-weld:	4.68	14.46	1.40	8.40
DNVGL-RP-C203:	4.14	------	3.09	------
X-shell-in plane bending-weld:	3.36	------	1.85	------
X-solid-in plane bending-weld:	3.37	------	1.76	------
DNVGL-RP-C203:	------	10.33	------	6.88
X-shell-out of plane bending-weld:	------	9.74	------	4.92
X-solid-out of plane bending-weld:	------	9.38	------	5.29

3.3. Comparison of SCFs obtained from the FEA against those estimated from DNVGL-RP-C203
The results shown on Table 9 and Table 10 demonstrate that, for the axial load case, the SCFs obtained from the FEA are conservative with regards to the values estimated from the parametric equations as given in DNVGL-RP-C203 [3], except at the chord "crown" location where the SCF obtained from the FEA either approach, as in the case of the welded tubular T joint, or surpass, as in the case of the welded tubular X joint, the value estimated from the parametric equations.

Table 9. Results-T joint, SCFs.

	CC	CS	BC	BS
DNVGL-RP-C203:	4.68	15.52	2.38	9.47
T-solid-axial-weld:	4.64	14.29	1.18	8.34
DNVGL-RP-C203:	4.14	------	3.09	------
T-solid-in plane bending-weld:	3.32	------	1.70	------
DNVGL-RP-C203:	------	10.98	------	7.31
T-solid-out of plane bending-weld:	------	9.91	------	5.49

Table 10. Results-X joint, SCFs.

	CC	CS	BC	BS
DNVGL-RP-C203:	3.18	22.02	2.38	12.15
X-solid-axial-weld:	4.68	14.46	1.40	8.40
DNVGL-RP-C203:	4.14	------	3.09	------
X-solid-in plane bending-weld:	3.37	------	1.76	------
DNVGL-RP-C203:	------	10.33	------	6.88
X-solid-out of plane bending-weld:	------	9.38	------	5.29

4. Discussion and conclusions

With reference to the importance of the presence of the weld geometry with regards to the FEA of tubular joints, the comparison of the results from the FE models ignoring and acknowledging the presence of weld geometry has shown that the FE models acknowledging the presence of weld geometry achieved higher SCFs than their counterpart. At the locations where the SCFs achieved their lowest values the trend becomes more apparent and is not in line with the results reported by K. Hectors and

De Waele [5] where the authors achieved higher SCFs from the FE models ignoring the presence of weld geometry. The set of FE models ignoring the presence of weld geometry presented in [5] had the extrapolation points located directly from the outer surface intersection of the brace and chord members and, thereby, ignoring the presence of the weld toe locations. For the purposes of this paper, the locations of the extrapolation points were implemented according to the recommendations given in DNVGL-RP-C203 [3] and as shown in Figure 3 on both the FE models ignoring and acknowledging the presence of weld geometry, that is by considering the presence of the weld toe locations. Nonetheless, and as corroborated in [5], it is undeniable that the presence of weld geometry has a major effect on the SCFs and, therefore, it is recommended that when performing the FEA of welded tubular joints the weld geometry should be implemented during the design stage and, more importantly, during structural integrity assessment projects in order to ensure the safe operation of offshore structures.

Concerning the suitability of shell and solid elements with regards to the FEA of welded tubular joints, the comparison of the results from the FE models using shell and solid elements has shown that the SCFs obtained from the FE models using the second order solid elements are lower than those achieved by the FE models using the first order shell elements at all the locations of interest, except at the brace "saddle" location where the opposite occurs. The lower SCFs obtained from the FE models using the second order solid elements are in line with the findings reported by K. Hectors and W. De Waele [5] where a similar tendency was encountered. Since solid elements represent more accurately the geometry of welded tubular joints, it is reasonable to assume that the results obtained from the FE models using solid elements are more representative of the true stresses experienced throughout the joint intersection and a further experimental study is recommended in order to confirm this finding.

With reference to the correlation between the standards AWS D1.1 [4] and DNVGL-RP-C203 [3] with regards to the minimum size of the weld geometry, the comparison of the SCFs obtained from the FEA against those estimated from the parametric equations as given in DNVGL-RP-C203 [3] has shown that, for the axial load case and at the chord "crown" location, the SCF obtained from the FEA either approach the value as estimated from the parametric equations, as in the case of the welded tubular T joint, or surpass the value as estimated from the parametric equations, as in the case of the welded tubular X joint. This finding would imply that the minimum size of the weld geometry as specified in AWS D1.1 [4] is insufficient at the chord "crown" location and, therefore, a further experimental study is recommended in order to validate the results obtained from the FE models presented in this paper. Furthermore, the recommended experimental study should be extended to include the welded tubular K and KT joint types.

References

[1] L. S. Etube, *Fatigue and Fracture Mechanics of Offshore Structures,* 2001.

[2] The British Standards Institution BSi, *BS EN ISO 19902:2007+A1:2013, Petroleum and natural gas industries - Fixed steel offshore structures,* 2013.

[3] DNVGL-RP-C203, *Recommended Practice, Fatigue design of offshore steel structures,* 2016.

[4] American Welding Society (AWS), *AWS D1.1/D1.1M:2010 Structural Welding Code - Steel 24th Edition,* 2020.

[5] K. Hectors and W. De Waele, *Influence of weld geometry on stress concentration factor distributions in tubular joints,* 2020.

[6] Ansys Inc., *Ansys Mecahnical APDL Documentation, Element Reference,* 2020.

[7] National Agency for Finite Element Methods and Standards (NAFEMS), *How To Use Beam, Plate and Shell Elements,* 2006.

[8] Ansys Inc., *Ansys Mecahnical APDL Documentation, Structural Analysis Guide,* 2020.

[9] R. D. Cook, D. S. Malkus, M. E. Plesha and R. J. Witt, *Concepts and Applications of Finite Element Analysis,* 2002.

[10] Ansys Inc., *Ansys Mecahnical APDL Documentation, Contact Technology Guide,* 2020.

Appendix

A.1. Plots-results from FE models ignoring and acknowledging weld geometry

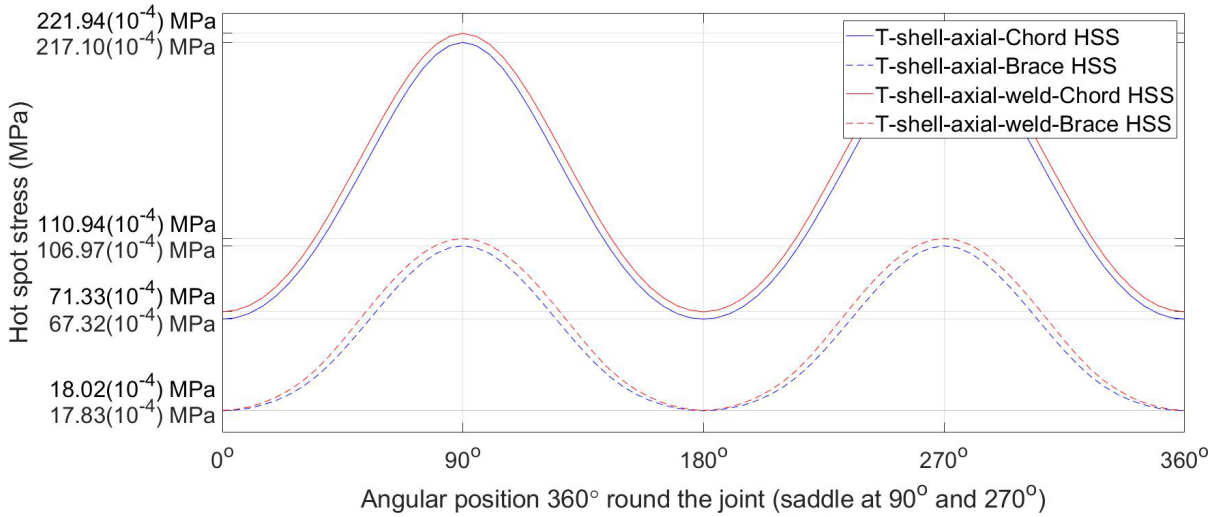

Figure 8. T-shell-axial vs T-shell-axial-weld, hot spot stresses.

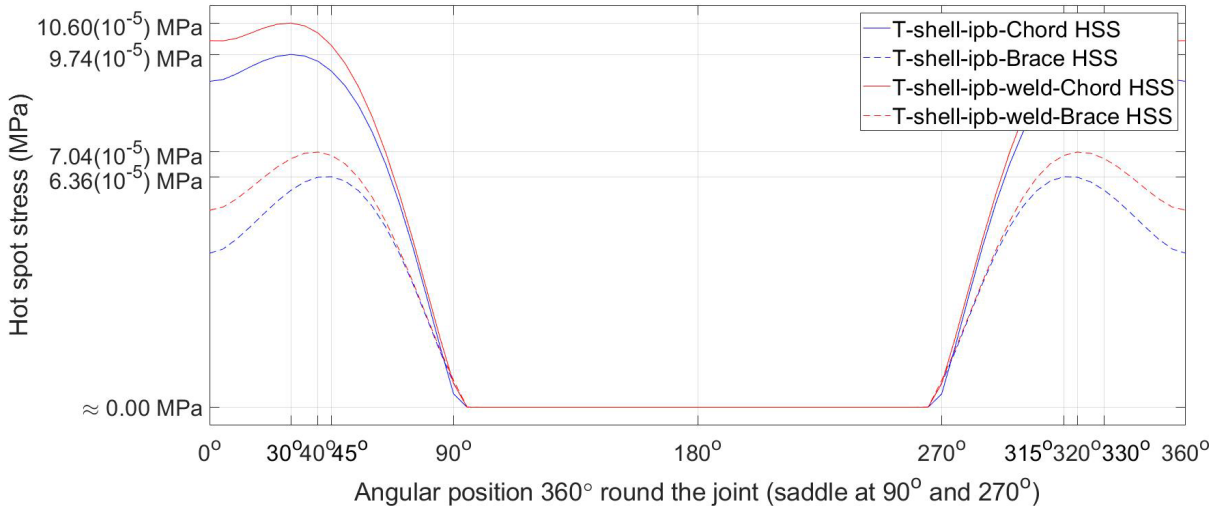

Figure 9. T-shell-in plane bending vs T-shell-in plane bending-weld, hot spot stresses.

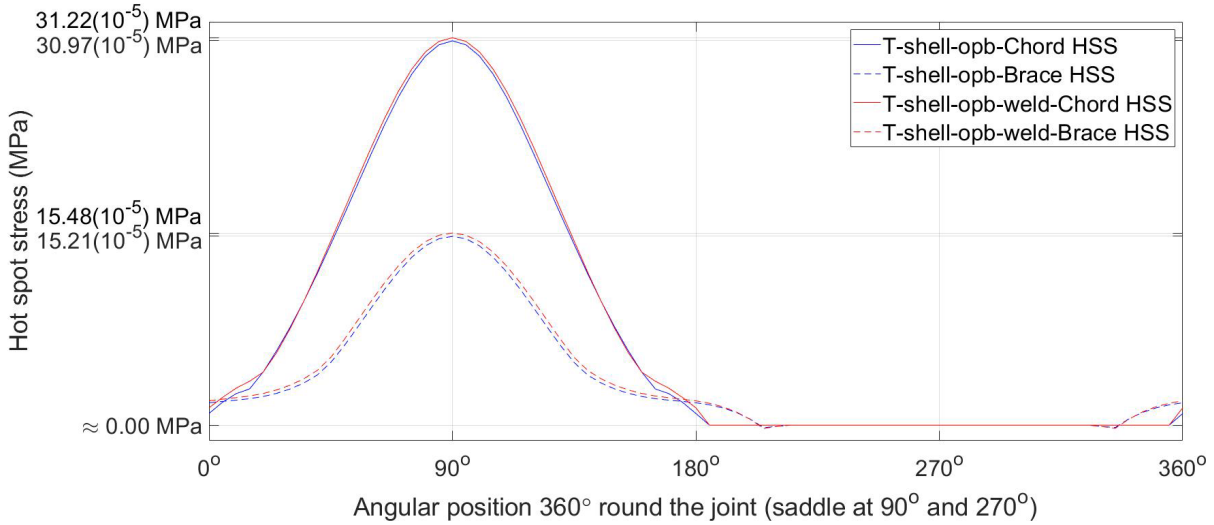

Figure 10. T-shell-out of plane bending vs T-shell-out of plane bending-weld, hot spot stresses.

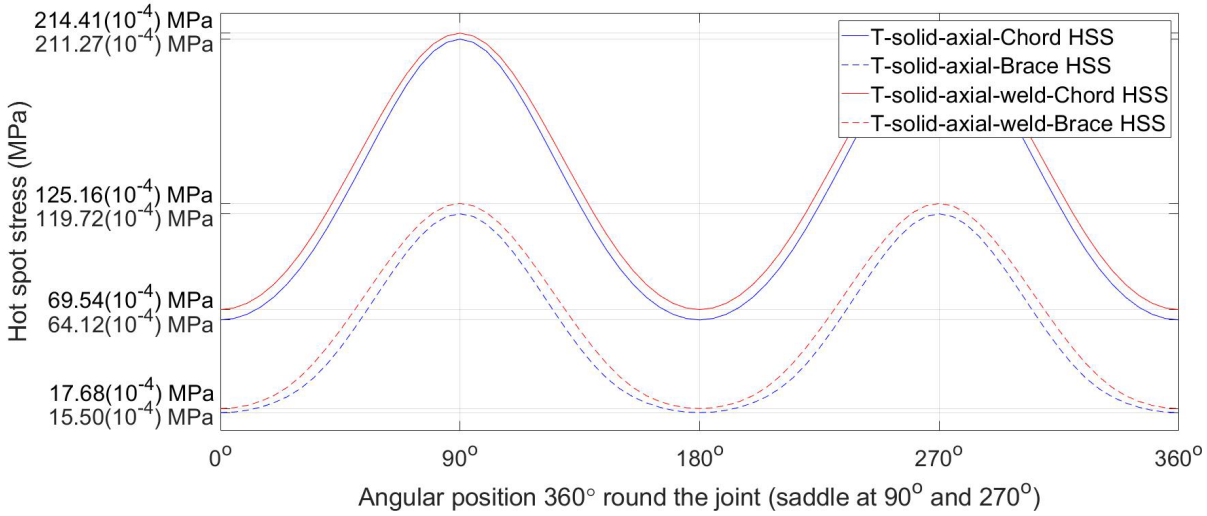

Figure 11. T-solid-axial vs T-solid-axial-weld, hot spot stresses.

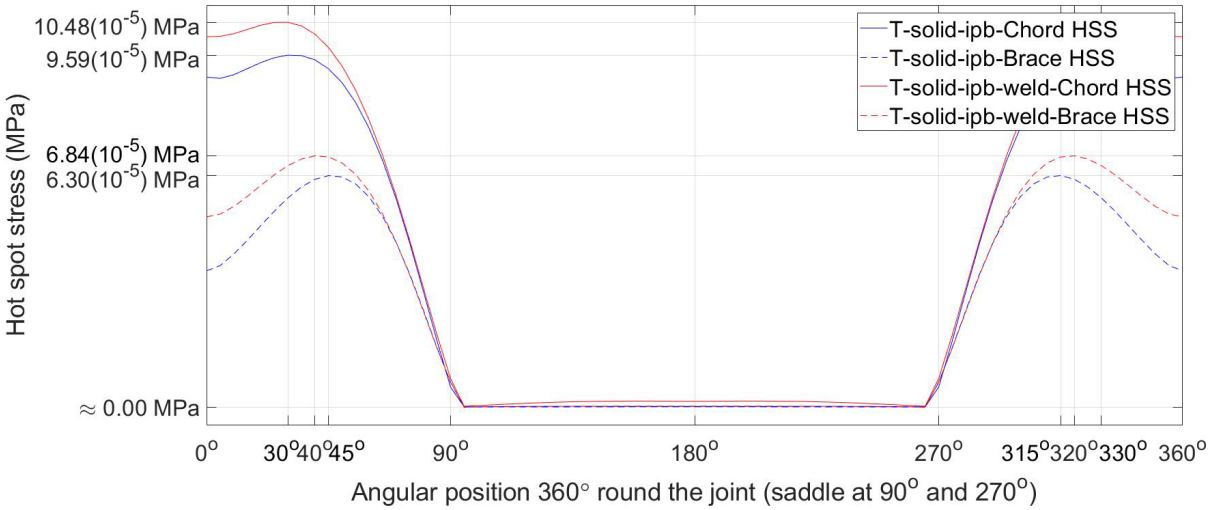

Figure 12. T-solid-in plane bending vs T-solid-in plane bending-weld, hot spot stresses.

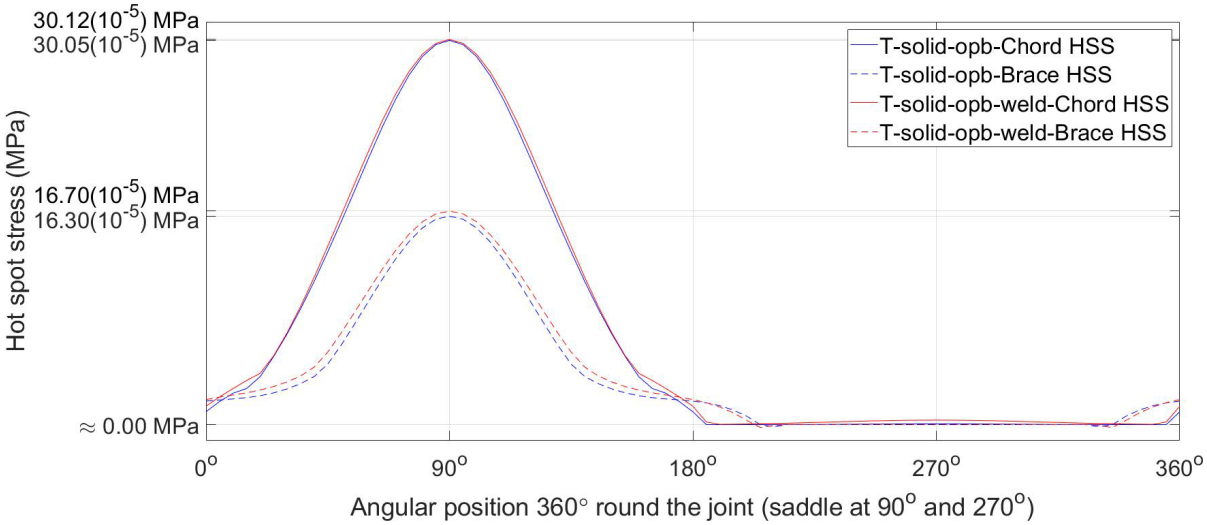

Figure 13. T-solid-out of plane bending vs T-solid-out of plane bending-weld, hot spot stresses.

A.2. Plots-results from FE models using shell and solid elements

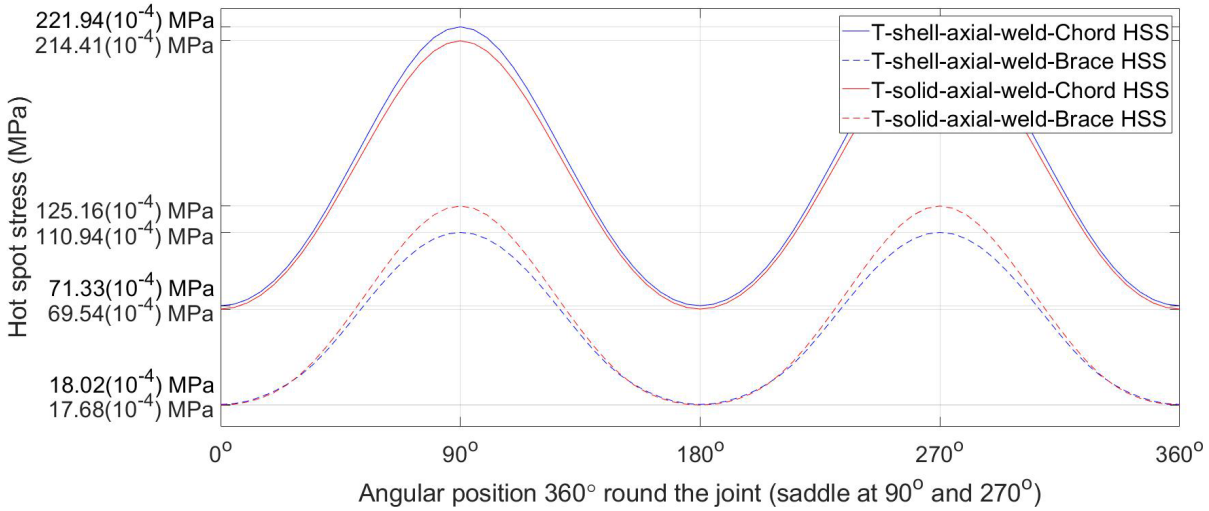

Figure 14. T-shell-axial-weld vs T-solid-axial-weld, hot spot stresses.

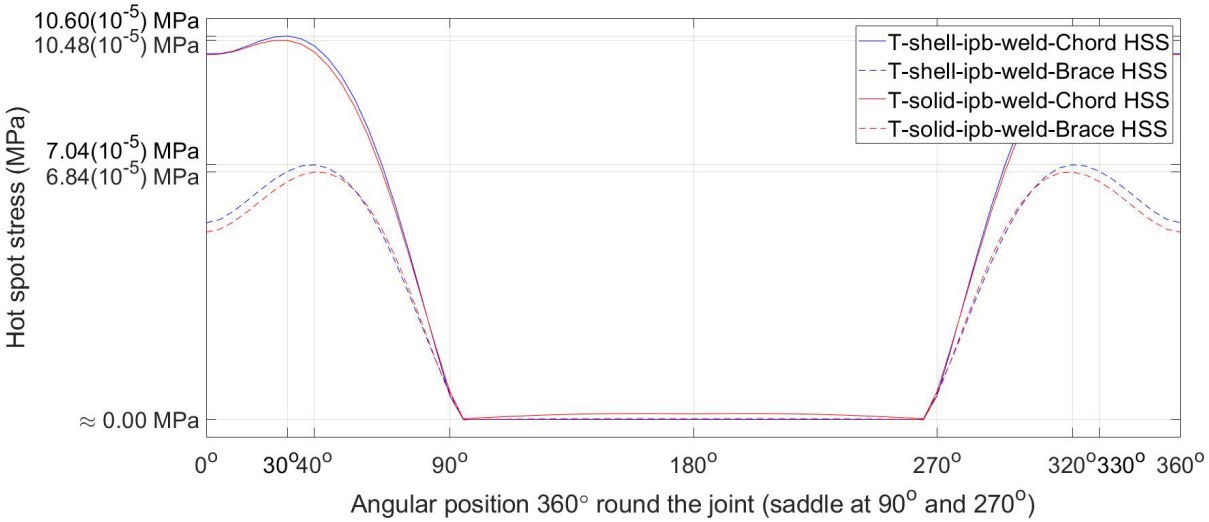

Figure 15. T-shell-in plane bending-weld vs T-solid-in plane bending-weld, hot spot stresses.

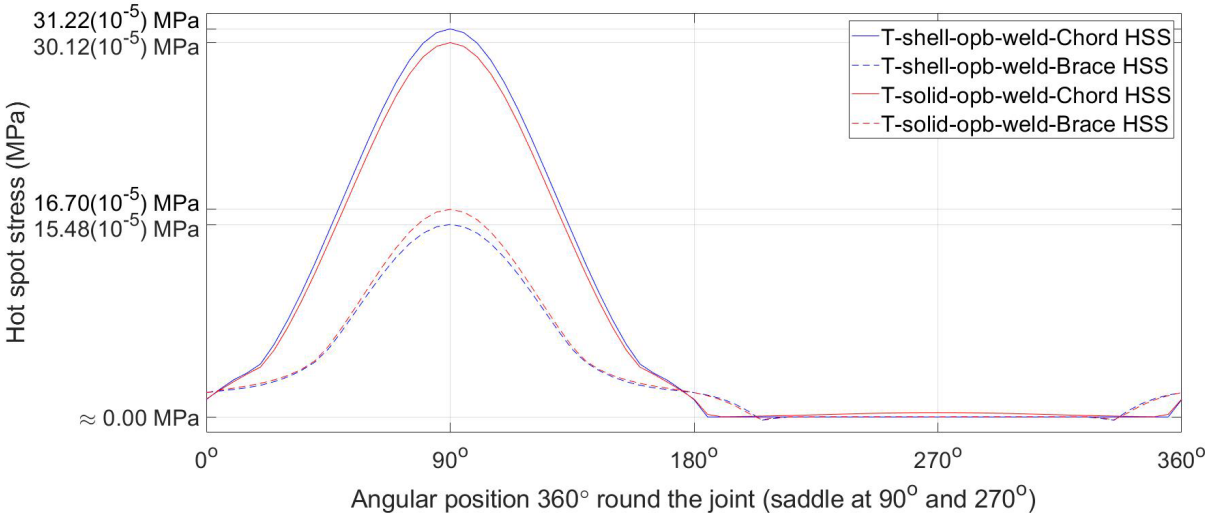

Figure 16. T-shell-out of plane bending-weld vs T-solid-out of plane bending-weld, hot spot stresses.

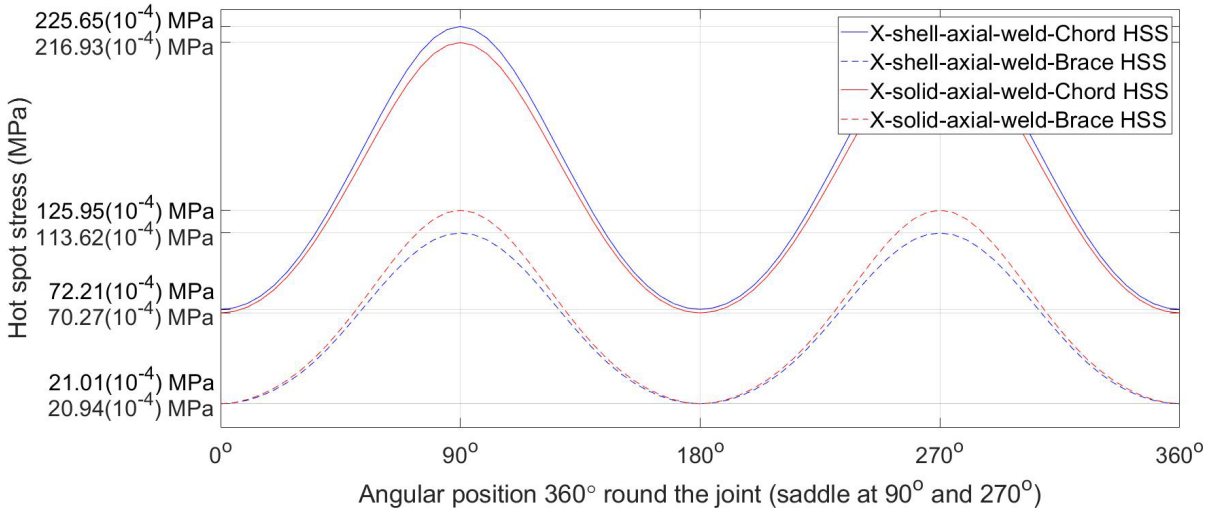

Figure 17. X-shell-axial-weld vs X-solid-axial-weld, hot spot stresses.

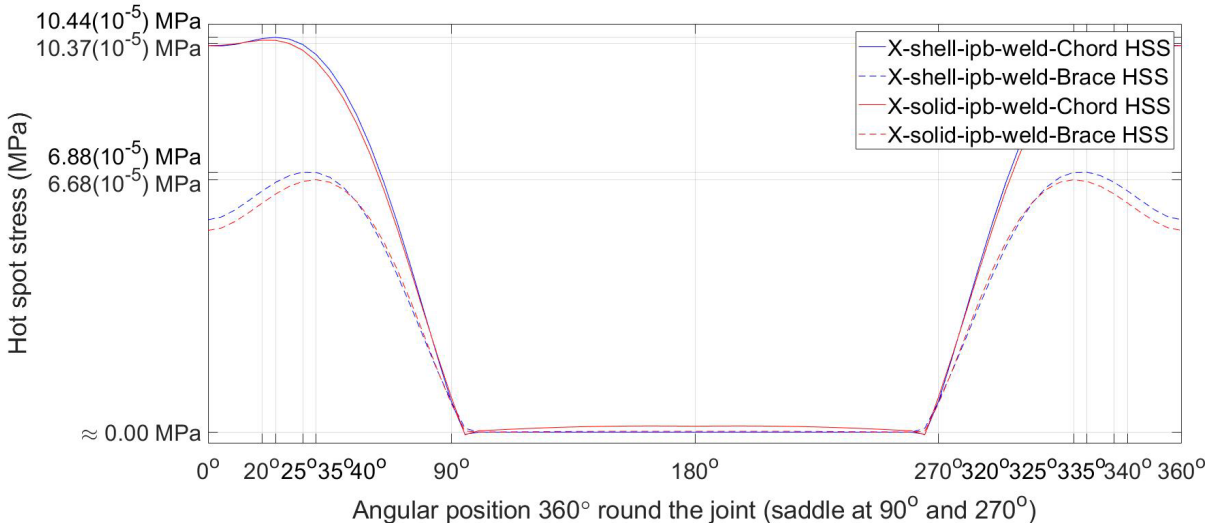

Figure 18. X-shell-in plane bending-weld vs X-solid-in plane bending-weld, hot spot stresses.

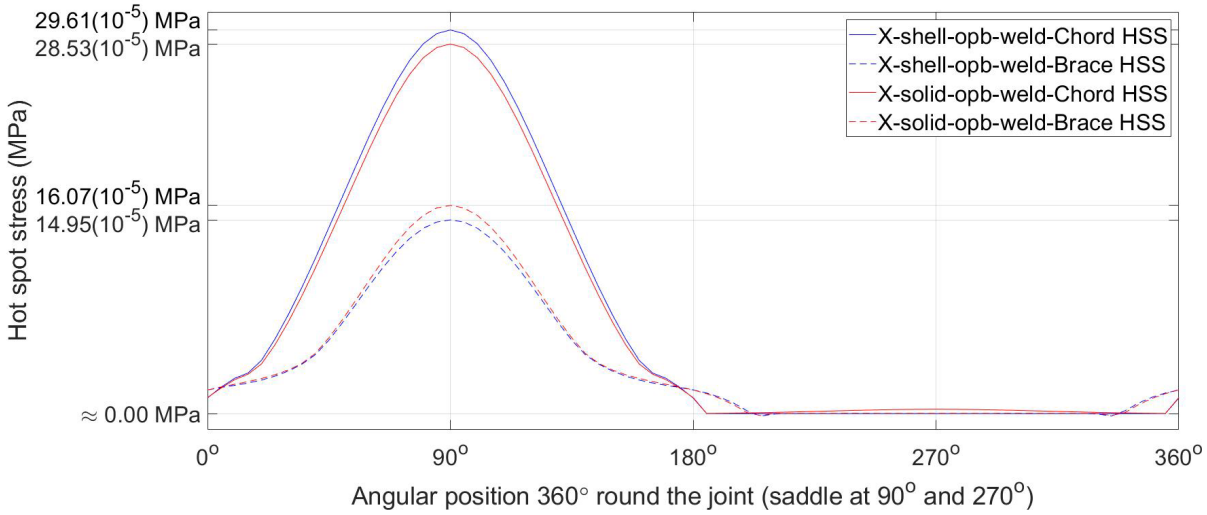

Figure 19. X-shell-out of plane bending-weld vs X-solid-out of plane bending-weld, hot spot stresses.